PHYSICAL REVIEW A VOLUME 17, NUMBER 2 FEBRUARY 1978

Study of the photodetachment cross section of F^-

T. N. Rescigno and C. F. Bender
Theoretical Atomic and Molecular Physics Group, University of California, Lawrence Livermore Laboratory, Livermore, California 94550

B. V. McKoy
A. A. Noyes Laboratory of Chemical Physics, California Institute of Technology, Pasadena, California 91125
(Received 6 July 1977)

The photodetachment cross section of F^- is calculated using the method of Stieltjes imaging. This technique constructs the photodetachment cross section from the finite number of transition energies and oscillator strengths obtained in a calculation employing discrete basis functions only. The cross sections are obtained at various levels of approximation which assess the importance of the coupling between channel components and of correlation effects. These effects are not found to play an important role in the determination of absorption cross sections by the Stieltjes-imaging method for the particular case under study. The calculated cross sections agree quite well with the measured cross sections.

I. INTRODUCTION

The availability of adequate tunable lasers has led to extensive experimental studies of the photodetachment cross sections of negative ions. These cross sections are important in the study of stellar spectra in identifying certain unexplained absorption continua,[1] and in our own atmosphere photodetachment of negative ions by sunlight is an important process.[2] Photodetachment also plays an important role in the modeling of various gas lasers.

Theoretical studies of photodetachment have concentrated primarily on atomic systems since the continuum eigenfunction of the photodetached system is numerically simple to generate.[3] In contrast there has been very limited progress in the study of photodetachment of molecular negative ions primarily because of the difficulties associated with the construction of continuum eigenfunctions for molecules. In view of these difficulties, various procedures have been developed for constructing photoionization or photodetachment cross sections from the results of calculations which employ square-integrable basis functions exclusively. Of these methods, the Stieltjes-Tchebycheff moment approach has proven to be very flexible and capable of providing reliable results for both the discrete and continuum portions of the photoabsorption profiles.[4]

We have recently proposed an approximate procedure for applying the Stieltjes-Tchebycheff moment approach to molecules. This approach avoids the potentially spurious results which can arise from weakly interacting channel components through a physically motivated channel-decoupling procedure and can also provide a dense pseudospectrum without the need for extensive configuration-interaction (CI) calculation.[5] The total photoionization cross section of N_2 so obtained from the Stieltjes-Tchebycheff method with pseudospectra derived within these approximations agrees well with recent measurements.[5] To further assess these approximations and to identify any new features of the Stieltjes-Tchebycheff moment methods associated with applications to photodetachment, we have calculated the photodetachment cross section of F^-. Also this atomic system enables us to specifically test the effect of decoupling of some channel components, e.g., the $(2p)^6 \rightarrow (2p)^5(\epsilon s)$ and $(2p)^6 \rightarrow (2p)^5(\epsilon d)$ components, and to introduce some correlation effects into both the initial- and final-state wave functions. The shape of the calculated cross section is found to agree well with both the measured cross sections and those of previous calculations. The magnitude of the calculated cross section is generally larger than the measured value, but this could be due in part to difficulties in the absolute determination of the cross section.

The Stieltjes imaging method is briefly described in Sec. II and a description of the procedures used to generate the pseudospectra is given in Sec. III. Some discussion of the computational methods is given in Section IV and the numerical results are presented and compared with available experimental data and the results of other calculations in Sec. V. Section VI contains a brief conclusion.

II. REVIEW OF THE STIELTJES METHOD

The Stieltjes imaging method has been discussed in detail in previous publications[6] and hence only the pertinent aspects of the development are given here.

The interaction of unpolarized electric dipole radiation with an atom or molecule is described in terms of the polarizability function

$$\alpha(\omega)=\int_0^\infty \frac{df(\epsilon)}{\epsilon^2-\omega^2}\,, \tag{1}$$

defined as a Stieltjes integral over the oscillator strength distribution $df(\epsilon)$. In Eq. (1), ϵ is an excitation energy and

$$df(\epsilon)=\left(\sum_i f_i\,\delta(\epsilon_i-\epsilon)+g(\epsilon)\right)d\epsilon \tag{2}$$

is the oscillator strength for transitions into the interval ϵ to $\epsilon+d\epsilon$. The f_i and $g(\epsilon)$ are the discrete and continuum portions, respectively, of the oscillator strength distribution.

Equations (1) and (2) formally require the construction of the discrete and continuum eigenfunctions in order to obtain the dispersion and absorption cross sections, i.e., the real and imaginary components of $\alpha(\omega)$, respectively. Approximating $\alpha(\omega)$ by a finite sum over N discrete energies and f values of a standard bound-state calculation leads to a polarizability function with the wrong analytic structure, i.e.,

$$\alpha(\omega)\simeq\sum_{i=1}^{N}\frac{\tilde{f}_i}{\tilde{\epsilon}_i^2-\omega^2} \tag{3}$$

has no imaginary component for all ω. However, the Stieltjes imaging method proposed by Langhoff[6] bypasses this fundamental difficulty of obtaining continuum eigenfunctions through the use of the mathematical theory of moments. This stems from the fact that the so-called cumulative oscillator strength distribution $F(\epsilon)$,

$$F(\epsilon)=\int_0^\epsilon df(\epsilon) \tag{4}$$

is uniquely defined by its spectral moments

$$S(-k)=\int_0^\infty \epsilon^{-k}\,df(\epsilon),\quad k=0,1,\infty. \tag{5}$$

Although the excitation energies $\tilde{\epsilon}_i$ and discrete-oscillator strengths $\tilde{f}_i$ obtained from a conventional bound-state calculation are unphysical and basis-set dependent, they can provide convergent approximations to the spectral moments of the oscillator-strength distribution in the form

$$S(-k)\simeq\tilde{S}(-k)=\sum_{i=1}^{N}\tilde{\epsilon}_i^{-k}\tilde{f}_i,\quad k=0,\ldots,2n-1. \tag{6}$$

These moments are, in principle, observable physical quantities. In practice, N pairs of $(\tilde{\epsilon}_i, \tilde{f}_i)$ provide a smaller number of converged moments $\tilde{S}(-k)$, i.e., $n\ll N$ in Eq. (6). However, from the theory of Stieltjes, the n pairs of parameters $(\epsilon_\alpha, f_\alpha)$ which solve the generalized quadrature problem associated with the *exact* values of the $2n$ sequential moments, i.e.,

$$S(-k)=\sum_{\alpha=1}^{n}\epsilon_\alpha^{-k}f_\alpha,\quad k=0,\ldots,2n-1\,, \tag{7}$$

provide a principal representation of the oscillator-strength distribution which can be used to construct an n-term histogram approximation to the cumulative oscillator strength in the form[6]

$$F(\epsilon)\simeq F^{(n)}(\epsilon)=\sum_{\epsilon_\alpha<\epsilon} f_\alpha,\quad \epsilon_\alpha\neq\epsilon\,. \tag{8}$$

The histogram of Eq. (8) rigorously bounds the correct distribution through the Tchebycheff inequalities

$$F^{(n)}(\epsilon_\alpha-0)<F(\epsilon_\alpha)<F^{(n)}(\epsilon_\alpha+0)\,, \tag{9}$$

and converges to $F(\epsilon)$ in the limit $n\to\infty$. In the Stieltjes imaging method of Langhoff the approximate moments, $\tilde{S}(-k)$ of Eq. (6), are used in Eq. (7) and the resulting moment equations solved for the n points and weights $(\tilde{\epsilon}_\alpha, f_\alpha)$. These points and weights are then used to obtain an approximation to the cumulative oscillator strength in the form of an n-term histogram

$$\tilde{F}^{(n)}(\epsilon)=\sum_{\tilde{\epsilon}_\alpha<\epsilon}\tilde{F}_\alpha,\quad \tilde{\epsilon}_\alpha\neq\epsilon\,. \tag{10}$$

With these approximate spectral moments $\tilde{S}(-k)$ the bounds of Eq. (9) are weakened.

To obtain an approximation to the differential oscillator-strength distribution $g(\epsilon)$ it is necessary to differentiate the cumulative histogram of Eq. (10). Following Stieltjes, approximations to the continuum oscillator strength can be obtained at the successive points

$$\tilde{\omega}_\alpha=\tfrac{1}{2}(\tilde{\epsilon}_{\alpha+1}-\tilde{\epsilon}_\alpha)\,, \tag{11}$$

from the slopes of the straight-line segments connecting adjacent Stieltjes values of the cumulative histogram $\tilde{F}^{(n)}(\epsilon)$ in the form

$$g(\tilde{\omega}_\alpha)=\tfrac{1}{2}(\tilde{f}_\alpha+\tilde{f}_{\alpha+1})/(\tilde{\epsilon}_{\alpha+1}-\tilde{\epsilon}_\alpha)\,. \tag{12}$$

More recently, the Stieltjes moment approach has been extended to the use of arbitrarily large numbers of spectral moments and an improved Stieltjes-Tchebycheff derivative approach, which gives continuous photoabsorption profiles has been introduced.[4,7] These additional procedures have yielded highly satisfactory results in several other problems including application to molecular nitrogen.[5] However, the photodetachment cross sections presented in this paper will be those derived from the Stieltjes imaging method. It has been our experience that there is generally a range of n values [Eq. (7)] over which mutually compatible Stieltjes image points can be obtained.

This range was found to be between five and nine for the present work. Calculations with smaller n values often fail to give the detailed structure of the cross section, while too high an n value gives results which begin to reveal the underlying discrete nature of the pseudospectra.

The Stieltjes-Tchebycheff moment analysis provides the basis for obtaining photoionization cross sections from the results of a calculation with discrete basis functions and thus entirely avoids the need for many-electron continuum wave functions.

III. GENERATION OF PSEUDOSPECTRA

The only photodetachment channel open in F^- for the energy range of interest here corresponds to $1s^22s^22p^6(^1S) \rightarrow 1s^22s^22p^5ks(^1P)$ and $1s^22s^22p^5kd(^1P)$. This threshold occurs at approximately 3.5 eV and is about 20 eV below the threshold for the next channel, $1s^22s^22p^6(^1S) \rightarrow 1s^22s2p^6kp(^1P)$. We thus need only obtain the pseudospectra appropriate to the ks and kd final continuum states.

A fairly large number of discrete excitation energies and oscillator strengths $(\tilde{\epsilon}_i, \tilde{f}_i)$ is required to provide a sufficient number of converged spectral moments $\tilde{S}(-k)$, and hence a suitable approximate principal pseudospectrum $(\tilde{\epsilon}_\alpha, \tilde{f}_\alpha)$. These pseudospectra will be obtained for F^- in three different approximations. First a set of N orbitals is obtained from a diagonalization of the static-exchange potential of the residual neutral core. The ϕ_{ns} and ϕ_{nd} orbitals are clearly uncoupled in this model and hence correspond to a complete decoupling of the ks and kd channel components. These one-electron eigenfunctions are then coupled to the core orbitals to produce the dipole-allowed final ^1P states. These states provide the discrete excitation energies and oscillator strengths $(\tilde{\epsilon}_i, \tilde{f}_i)$ used to construct the spectral moments $\tilde{S}(-k)$. Since this approach involves computations with SCF Hamiltonians the pseudospectra can be obtained from the diagonalization of relatively small matrices.[5]

Physically the above choice of the effective one-particle Hamiltonian implies that the pseudo-orbitals are eigenfunctions of the V_{n-1} potential defined by the initial SCF solution of F^-. This choice has the advantage of including important final-state interaction effects, since the core orbitals of the neutral atom are allowed to adjust to the presence of the photoejected electron. This means that although the final pseudostates are formally uncoupled, the final pseudospectra can contain certain correlation effects.[8]

The other two approximations for generating the pseudospectra include coupling between the channel components ϕ_{ns} and ϕ_{nd}, and some correlation effects in the initial- and final-state wave functions. First the virtual orbitals or particle states of the F^- Hartree-Fock Hamiltonian are used to diagonalize the total Hamiltonian over all singly excited configurations of the type $1s^22s^22p^6 \rightarrow 1s^22s^22p^5\phi_{ns}$ and $1s^22s^22p^5\phi_{nd}$. This corresponds to the singly excited configuration-interaction method (SECI) or the Tamm-Dancoff approximation (TDA). These pseudostates hence include explicit coupling of the channel components. The initial state of F^- is still described in the Hartree-Fock model and is hence uncorrelated. Beyond this, the work of Kelly and Simons[9] on argon suggests that ground-state correlations involving excitation of a single pair of electrons from the $(2p)^6$ shell into d orbitals are the dominant ones for the $2p \rightarrow \epsilon d$ photoionization. Since this type of excitation, along with those of the type $2p^6 \rightarrow 2p^4(ns)^2$, are those included in the description of the excitation spectrum of F^- in the random-phase approximation (RPA), we also generate the pseodospectra in this approximation. Advantages of RPA pseudospectra are that certain spectral moments are well approximated, e.g., $S(0)$, and that the length and velocity forms of the oscillator strength are formally equivalent. These and other details of the RPA or time-dependent Hartree-Fock approximation are given elsewhere.[10] In none of our approximations have we included excitations from the occupied $1s$ and $2s$ orbitals.

IV. COMPUTATIONAL ASPECTS

An SCF wave function for the ^1S ground state of F^- is obtained in a contracted basis set of [16s, 6p, 7d] Gaussian functions. The total energy in this basis is -99.446 a.u. The first two s functions are taken from Dunning's [3s] contraction[11] and these are augmented with 14 additional functions with exponents ranging from 3.0 to 0.004. The p basis consists of Dunning's 2p contraction with four additional functions and the d basis, which contains the x^2, y^2, z^2, xz and yz components, has exponents ranging from 1.87 to 0.005. It was found to be very important to use a p basis of this size to adequately describe the tail region of the 2p orbital. While the additional functions needed to describe this region have little effect on the total energy, they do have a large effect on the computed oscillator strengths. The orbital energy of the 2p orbital is -0.1797 a.u.

The s and d virtual orbitals of this SCF potential are then used to diagonalize the static-exchange potential of the $1s^22s^22p^5$ core of F^-. The resulting eigenfunctions of the V_{n-1} potential are coupled with the core of F^- to produce the appropriate ^1P

TABLE I. Pseudospectrum of excitation energies and oscillator strengths for the photodetachment of F^- in the RPA.[a]

$\tilde{\epsilon}_i$ [b]	$\tilde{f}_i$ [c]
0.126 408	0.007 530
0.137 940	0.001 218
0.141 231	0.027 194
0.173 786	0.050 842
0.175 624	0.022 277
0.239 417	0.055 265
0.276 197	0.157 784
0.365 125	0.084 354
0.546 017	0.763 973
0.593 360	0.171 271
0.986 815	0.086 534
1.234 125	2.422 862
1.648 825	0.063 039
2.749 278	0.109 529
2.868 843	2.027 122
4.593 853	0.036 207
6.785 630	0.792 594
7.729 941	0.008 054
1.327 905	0.003 012
2.436 401	0.004 599
8.174 583	0.000 137

[a] All quantities in atomic units.

[b] The RPA excitation energies shifted to the experimental threshold.

[c] These f numbers contain all degeneracy factors.

pseudostates. We also use these virtual orbitals to carry out the TDA and RPA calculations which provide 21 discrete excitation energies and oscillator strengths. Of these, 14 correspond to the $1s^22s^22p^5ks$ channel component and seven to the $1s^22s^22p5kd$.

With these pseudospectra the Stieltjes moment analysis provides stable results with up to 16 spectral moments. Analysis with a larger number of moments lead to photodetachment cross sections which are unphysical and reveal the discrete nature of the original pseudospectra.

V. RESULTS

The discrete excitation energies and oscillator strengths derived from the calculated RPA spectrum are given in Table I. The excitation energies in this table are those of the RPA calculation shifted so that the first excitation energy agrees with the observed threshold for photodetachment. The first unshifted excitation energy is 5.01 eV and should approximate the energy of the $1s^22s^22p^5$ core of F^- plus an electron at almost zero energy. The difference between this and the observed threshold 3.44 eV[12] is primarily due to the energy difference between the $1s^22s^22p^5$ core of F^- and the F atom (recall that the 1s and 2s orbitals were frozen in these calculations). This shifted spectrum is also used in computing the oscillator strengths. We used the same procedure of shifting the excitation energies to the experimental threshold in our previous calculations on the photoionization cross sections of N_2.[5]

The spectral moments derived from the pseudospectrum in the static-exchange approximation and in the TDA are very close to those from the pseudospectrum of Table I. The spectral moments $\tilde{S}(0)$ and $\tilde{S}(-2)$, which should approximate the number of active electrons in the system, i.e., $(2p)^6$ and the static polarizability, respectively, have values of 6.9 and $13.00\alpha_0^3$. The overestimation of the sum rule is minor and in part due to the decoupling of the $(2p)^6$ system from the $(2s)^2$ subsystem. The calculated polarizability is considerably larger than the experimental estimate of $6.8\alpha_0^3$, but close to the uncoupled Hartree-Fock value of $12.2\alpha_0^3$.[13]

The photodetachment cross section of F^- obtained from Stieltjes imaging of the pseudospectrum of Table I is shown in Fig. 1. The cross sections plotted are those derived from fifth-, sixth-, seventh-, and eighth-order Stieltjes calculations. These calculations use 10, 12, 14, and 16 spectral moments, respectively, and hence yield an approximate principal pseudospectrum with 5, 6, 7, and 8 pairs of $(\tilde{\epsilon}_\alpha, \tilde{f}_\alpha)$. Calculations employing a larger number of spectral moments yield unphysical cross sections which reveal the underlying discrete nature of the pseudospectra.

In Fig. 1 we also plot the experimental data of Mandl[12] and the calculated cross sections of Ishihara and Foster.[3] The shape of our calculated

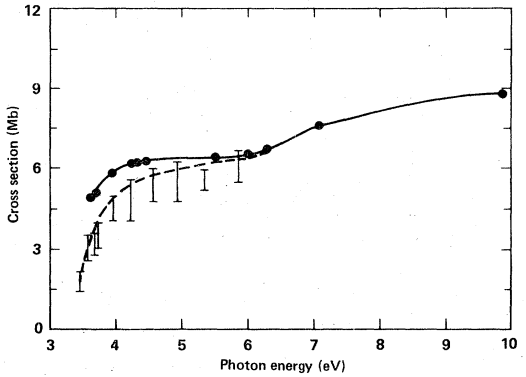

FIG. 1. Photodetachment cross sections for F^-. Present results are denoted by the solid curve which passes through the fifth through eighth-order Stieltjes image points (●). These results were obtained in the coupled random phase approximation (see text). Dashed curve (--), fully coupled theoretical results of Ishihara and Foster. The experimental points (I) are those of Mandl (Ref. 12).

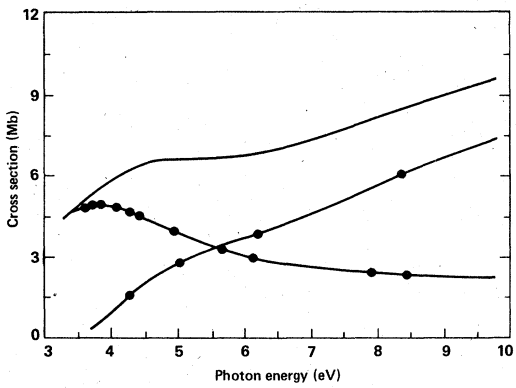

FIG. 2. Photodetachment cross sections for F^- in the uncoupled random phase approximation. The *ks* and *kd* channel components, obtained from the Stieltjes image points, as well as their sum, are shown separately. The lower of the two curves at threshold is the *kd* component.

cross section agrees well with the measured cross sections, but the calculated results are generally larger. In the threshold region this stems from the rapid rise of the calculated cross section compared with the measured values. Mandl suggests an uncertainty of ±25% for his measurements.[12] The calculated cross sections of Ishihara and Foster, who used many-body perturbation theory, also lie on the high side of Mandl's data. Additional experimental studies of the photodetachment cross section of F^- would be useful.

We do not present the total cross section obtained in the SCF and TDA approximations since they are very similar to those of Fig. 1. This simply reflects the earlier observation that the three approximations give similar values of the spectral components.

In Fig. 2 we show the cross sections for the $1s^22s^22p^6 \rightarrow 1s^22s^22p^5ks$ and $1s^22s^22p^5kd$ components separately. These cross sections are obtained by completely decoupling the two-channel components through two separate RPA calculations. We then use the Stieltjes-image method to obtain the partial photodetachment cross sections. The sum of these two partial cross sections is quite close to the cross section obtained with the *s* and *d* channels coupled. It is hence clear that this coupling is not an important effect in F^-.

VI. CONCLUSIONS

The Stieltjes imaging method has been used along with pseudospectra derived in the static-exchange approximation, configuration interaction with single excitations or TDA, and random-phase approximation (RPA) to study the photodetachment cross section of F^-. The resulting cross sections are quite similar both in magnitude and shape indicating that both the coupling between channel components and the effects of initial-state correlations are not important. The calculated cross sections also agree reasonably well with both the magnitude and shape of the measured cross sections.

These conclusions are important for molecular applications where such approximations can greatly simplify the calculation of photoionization cross sections. We also emphasize that the Stieltjes image method requires the use of discrete basis functions exclusively and hence avoids the computational difficulties associated with the construction of continuum functions for molecular systems.

ACKNOWLEDGMENTS

This work was performed under the auspices of the U.S. Energy Research and Development Administration under Contract No. W-7405-Eng-48. One of us (B.V.M.) also acknowledges support provided by a grant from the NSF.

[1]M. S. Vadya, Mem. R. Astron. Soc. 71, 249 (1967).
[2]L. M. Branscomb, Ann. Geophys. 20, 88 (1964); see also, H. S. W. Massey, *Negative Ions* (Cambridge U.P., Cambridge, 1976).
[3]T. Ishihara and T. C. Foster, Phys. Rev. A 9, 2350 (1974).
[4]See, for example, P. W. Langhoff, C. T. Corcoran, J. S. Sims, F. Weinhold, and R. M. Glover, Phys. Rev. A 14, 1042 (1976). References to earlier work on the Stieltjes moment methods can be found in this paper.
[5]T. N. Rescigno, C. F. Bender, V. McKoy, and P. W. Langhoff, J. Chem. Phys. (to be published).
[6]P. W. Langhoff, J. Sims, and C. T. Corcoran, Phys. Rev. A 10, 829 (1974).
[7]P. W. Langhoff and C. T. Corcoran, Chem. Phys. Lett. 40, 367 (1976); C. T. Corcoran and P. W. Langhoff, J. Math. Phys. 18, 651 (1977).
[8]M. Ya Amusya, N. A. Cherepkov, and L. V. Chernysheva, Sov. Phys.-JETP 33, 90 (1971); see also, J. R. Swanson and L. Armstrong, Phys. Rev. A 15, 661 (1977); and Ref. 9.
[9]H. P. Kelly and R. L. Simons, Phys. Rev. Lett. 30, 529 (1973).
[10]See, for example, T. Shibuya and V. McKoy, Phys. Rev. A 2, 2208 (1970).
[11]T. H. Dunning and P. J. Hay, in *Modern Theoretical Chemistry*, edited by H. F. Schaefer (Plenum, New York, 1976), Vol. 3.
[12]A. Mandl, Phys. Rev. A 3, 251 (1971).
[13]M. Yoshimine and R. P. Hurst, Phys. Rev. 135, A612 (1964).